CHAPTER IV
RESULTS AND DISCUSSIONS

This chapter began with a determination of the coherence length of superluminescent diode (SLD), used as low coherence light source in this research. Then, an image of step-height standard plate and a depth of the step were investigated by the discrete Fourier transform (DFT) and the continuous wavelet transform (CWT) for confirming 3-D surface profile constructing ability of optical coherence tomography (OCT). Also, the depth of a step of step-height standard plate was determined. Next, both DFT and CWT were used to image a cross-section of three stainless steel plates and then the root-mean-square roughness (R_q) was reported. A surface profile of these three stainless steel plate with and without transparent material cover was constructed and compared with each other. Finally, a thickness of the transparent material was calculated by using different positions between interferogram of inner surface and the one of transparent material surface.

The light beam, recorded by CCD camera, had a size of 4 × 3 mm in horizontal and vertical, respectively. Since the CCD camera had 640 horizontal pixels and 480 vertical pixels; therefore, each pixel of the CCD camera represented 6.25 × 6.25 μm image sizes. To avoid flare light, which reflected from neighbor CCD pixel, an average of 4 × 4 pixels would be considered as a surface area. Thus, the whole image had 160 × 120 values and each value contained an area size of 25 × 25 μm.

4.1 Coherence Length of SLD

The SLD, used in this research, had 830 nm of central wavelength and 15 nm of full-width at half-maximum (FWHM). The coherence length calculated from Eq.(2.24) was 20 μm. From Eq.(2.24):

$$L_C = \frac{2\ln 2}{\pi}\frac{\overline{\lambda}^2}{\Delta\lambda}.$$

Thus, the theoretical coherence length calculated by this equation is:

$$L_C = \frac{2\ln 2}{\pi}\frac{(830)^2}{15} = 20\ \mu\text{m}.$$

The coherence length can be also determined by FWHM of intensity signals of a plain mirror [2]. The intensity signals from a plain mirror, measured by the Michelson interferometer as shown in Figure 4.1, were analyzed by low-pass filter. Then, it was fitted by a Gaussian shape, as shown in Figure 4.2. The coherence length of this SLD, which relates to FWHM of the intensity signals, was 22 μm. This observed value agreed with the one from calculation. That means a minimum thickness of each layer of multi-layer sample, which could clearly separate by this SLD, should be 22 μm.

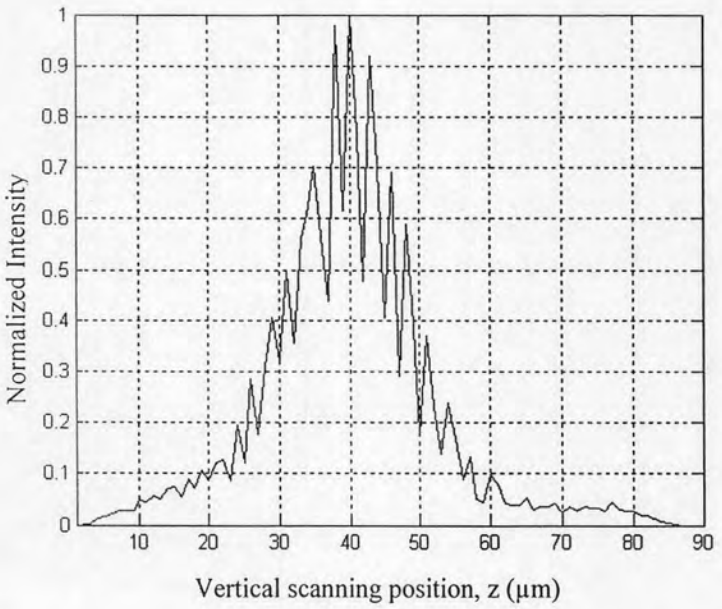

Figure 4.1: Intensity signals of plain mirror

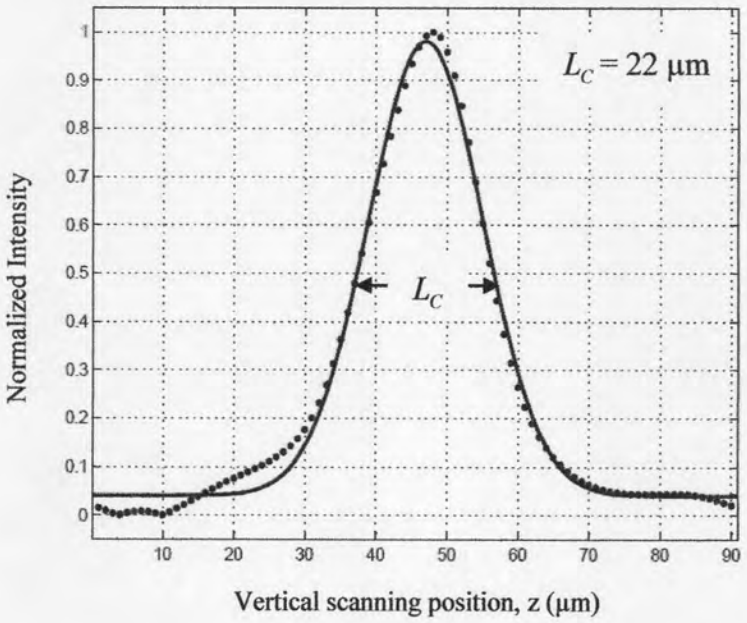

Figure 4.2: Coherence length of SLD light

4.2 Surface Profile of Step-height Standard Plate

To confirm an analyzing method in this research, a step-height standard plate was used as a standard sample for constructing its surface and calculating its depth of step. Both DFT and CWT was used to construct the surface profile of this step-height standard plate. The step-height standard plate from VLSI Standard Incorporated and its structure diagram are shown in Figure 4.3.

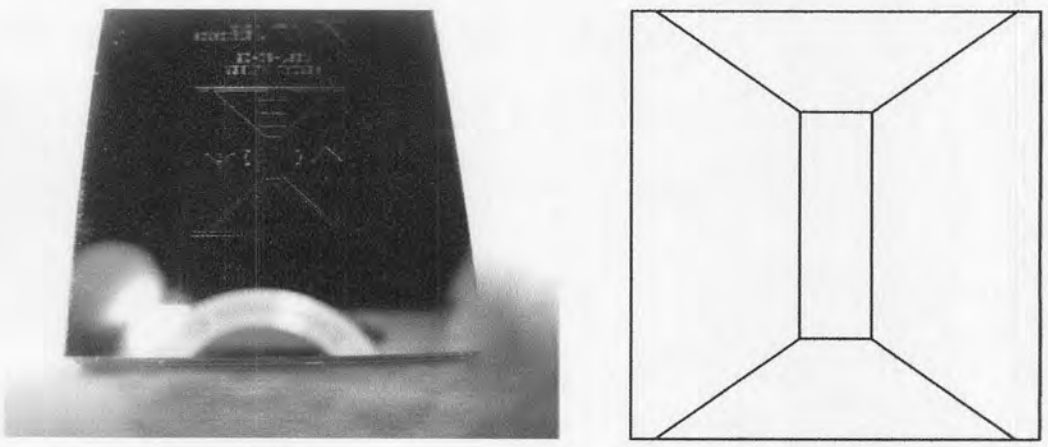

(a) (b)

Figure 4.3: (a) Picture of step-height standard plate and (b) its diagram

The example of interferogram of 4 × 4 pixels with noise filtering and its CWT spectrogram are shown in Figure 4.4.

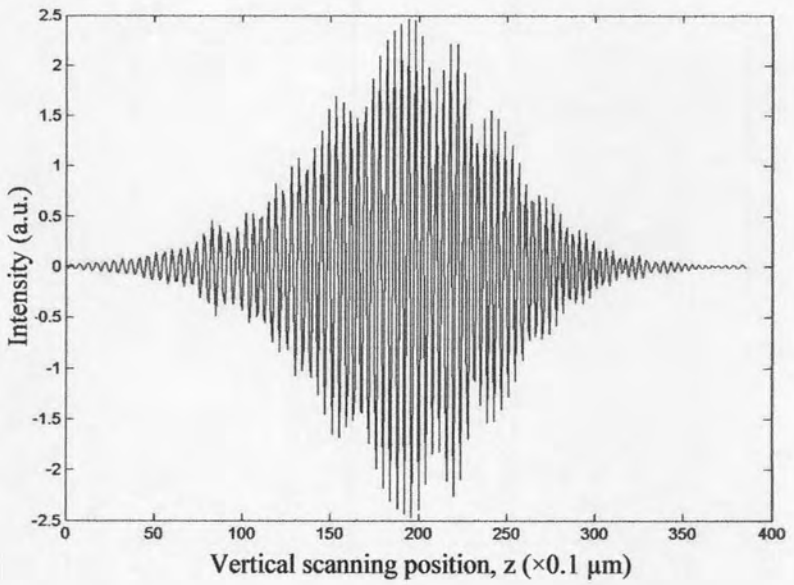

(a)

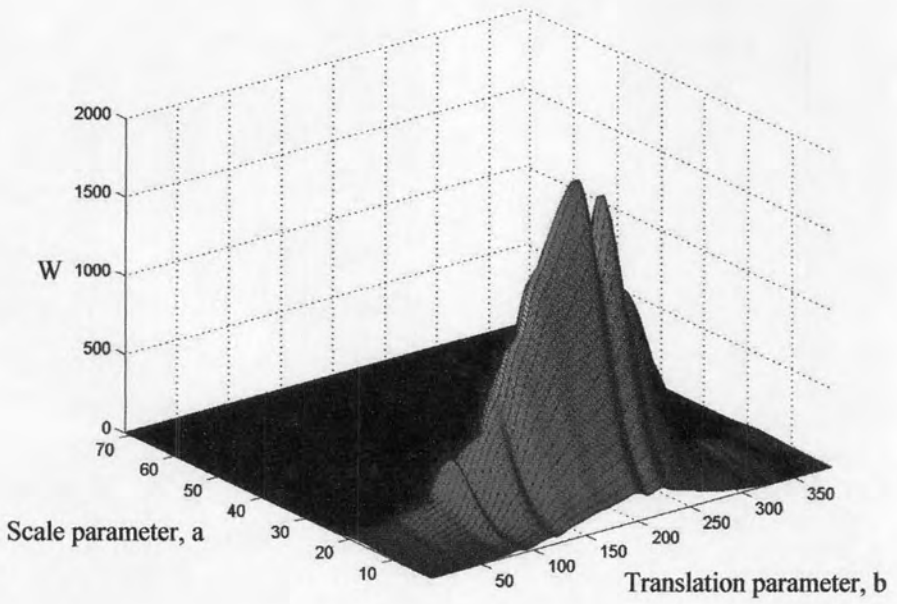

(b)

Figure 4.4: (a) Intensity signals in each vertical scanning step (b) its CWT spectrogram

Then, a maximum $W_{a\_\max,b\_\max}(z)$ of the CWT spectrogram was defined and the real position of surface height, z_R, was calculated by Eq.(2.31) as:

$$z_R = z_M - \frac{\overline{\lambda}}{4\pi}\varphi .$$

After the real position of surface height in the whole area of step-height standard surface was already defined by both DFT and CWT, the surface profile of step-height standard plate, constructed by both methods, are shown in Figure 4.5.

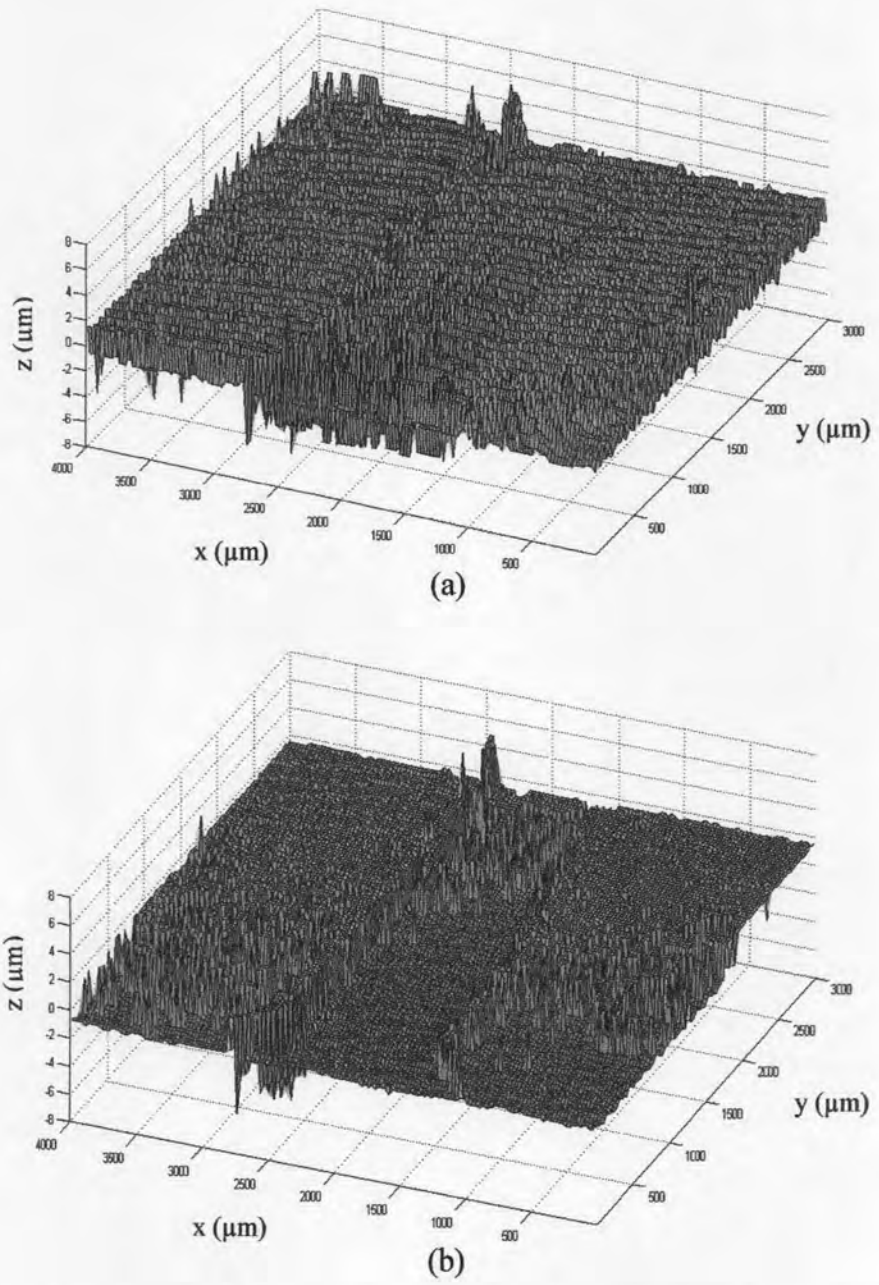

Figure 4.5: Surface profile of step-height standard plate by (a) DFT and (b) CWT

According to the surface profile of step-height standard plate, constructed with DFT and CWT, as shown in Figure 4.5, the constructed surface by CWT is closed to the real surface while DFT could not define the depth of standard surface. An error on a right corner, as shown in Figure 4.5 (b), might be caused by a tilt of the surface orientation. Because a shape of step-height standard plate is a square shape, a circular optical mount is not fit with the standard plate. The cross-section in one line of this standard plate is shown in Figure 4.6. By using CWT, the depth of a top and bottom surface of step-height standard plate in some different area could be calculated as in Table 4.1.

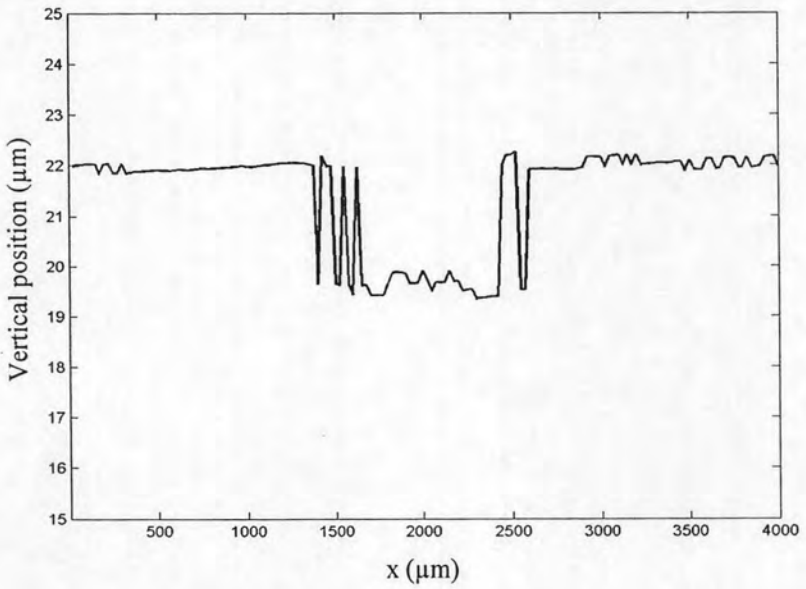

Figure 4.6: Cross-section of step-height standard plate

Table 4.1: The depth of step-height standard plate

No.	Mean of top position (μm)	Mean of bottom position (μm)	Calculated depth (μm)
1	21.464	19.463	2.001
2	21.510	19.556	1.954
3	21.535	19.576	1.959
4	21.605	19.568	2.037
5	21.726	19.591	2.135
6	21.840	19.671	2.169
7	21.777	19.654	2.123
8	21.853	19.644	2.209
9	21.931	19.568	2.363
10	21.871	19.605	2.266
11	21.914	19.841	2.073
12	21.929	19.932	1.997
13	21.872	19.884	1.988
14	21.893	19.858	2.035
15	21.810	19.866	1.944
16	21.844	19.887	1.957
17	21.927	19.953	1.974
18	21.905	19.983	1.922
19	21.923	19.845	2.078
20	21.975	19.870	2.105
Average			**2.064**
S.D.			**0.118**

In this experiment, an uncertainty of a system was obtained from the wavelength bandwidth ($\Delta\lambda$) of SLD, PZT stage and reference mirror. It also calculated by following the accreditation guideline [23].

According to manufacture data, the wavelength bandwidth of SLD was 0.015 μm. By assuming a rectangular distribution, the standard uncertainty of the bandwidth was given by $u_{\Delta\lambda} = \frac{0.015}{\sqrt{3}} = 0.009$ μm.

An error of the PZT stage could be compared with an input voltage that supply to this PZT stage. The maximum error in a distance, measured by Nation Institute of Metrology (Thailand) (NIMT), was 0.054 μm. The standard uncertainty using the rectangular distribution for this PZT stage was given by $u_{PZT} = \frac{0.054}{\sqrt{3}} = 0.031$ μm.

A roughness of the reference mirror, evaluated by NIMT, was 0.0006 μm. The standard uncertainty of the mirror roughness using the rectangular distribution was given by $u_{mirror} = \frac{0.0006}{\sqrt{3}} = 0.0004$ μm.

From the accreditation guideline [23], a combined uncertainty was given by:

$$u_C = \sqrt{u_{\Delta\lambda}^2 + u_{PZT}^2 + u_{mirror}^2} \tag{4.1}$$

Thus, the combined uncertainty of this OCT, used in this research, was 0.032 μm. For a level of confidence of 95.5% with coverage factor $k = 2$, an expanded uncertainty (U) of this system was expressed by:

$$U = k \times u_C \tag{4.2}$$

Thus, the uncertainty of this system at a level of confidence of 95.5% was 0.064 μm. A summary of various standard uncertainties is shown in Table 4.2.

Table 4.2: The standard uncertainty component

Source of uncertainty	Uncertainty value	Probability distribution	Standard uncertainty
Wavelength bandwidth	0.015 μm	Rectangular	0.009 μm
PZT stage	0.054 μm	Rectangular	0.031 μm
Roughness of mirror	0.0006 μm	Rectangular	0.0004 μm
Combined uncertainty	-	Normal	0.032 μm
Expanded uncertainty	-	Normal	0.064 μm

Therefore, an average depth from this experiment was 2.064 ± 0.064 μm. The average depth of this standard, measured by 3-D Non-Contact Surface Profiler SP-500 Series from Toray Engineering Co., Ltd, was 1.780 ± 0.019 μm. Because the SP-500 Series had a suitable slot for placing the standard plate, an orientation of the surface was not an effect on the measurement. While a sample holder for this research was not designed for using with this standard plate, the calculated depth by OCT was different from the SP-500 Series by 14.7%.

4.3 Cross-section of Stainless Steel Plate

A cross-section of three stainless steel plates (Sample No.1, No.2 and No.3) and their root-mean-square roughness (R_q) will be shown in this section. The cross-section of each sample was measured from 101st-104th (line 1), 201st-204th (line2), 301st-304th (line 3) and 401st-404th (line 4) vertical pixels, as shown in Figure 4.7.

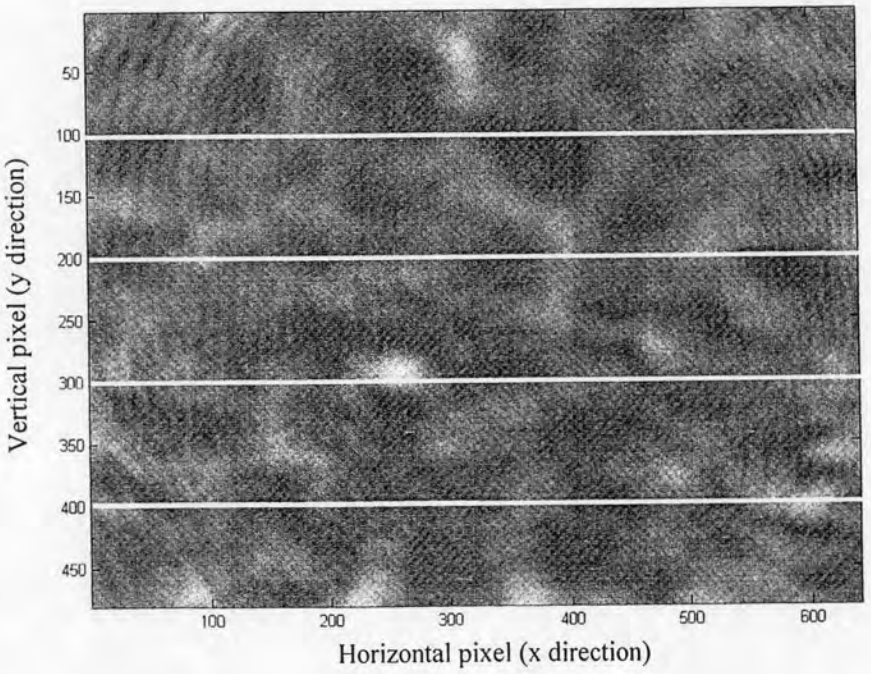

(a)

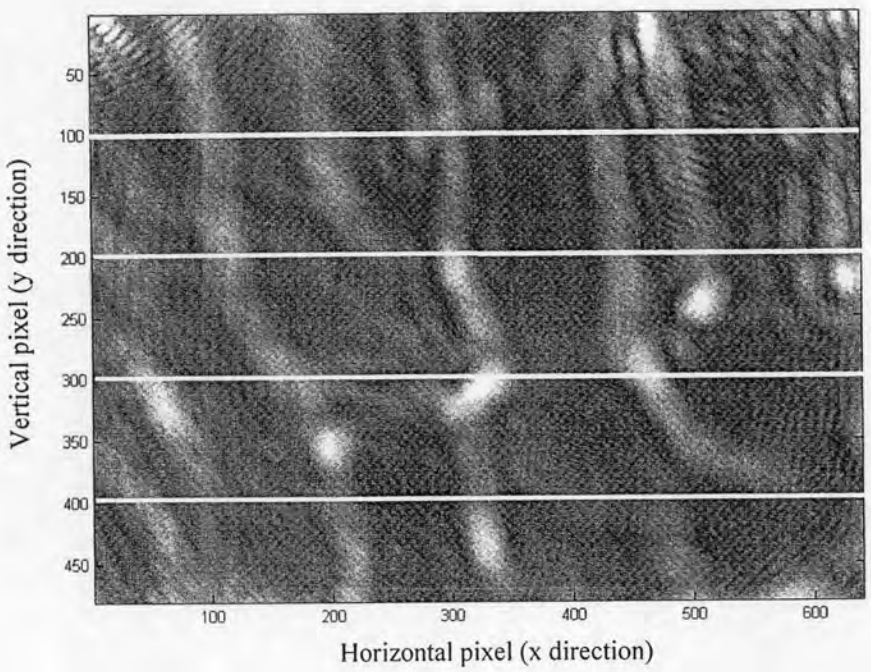

(b)

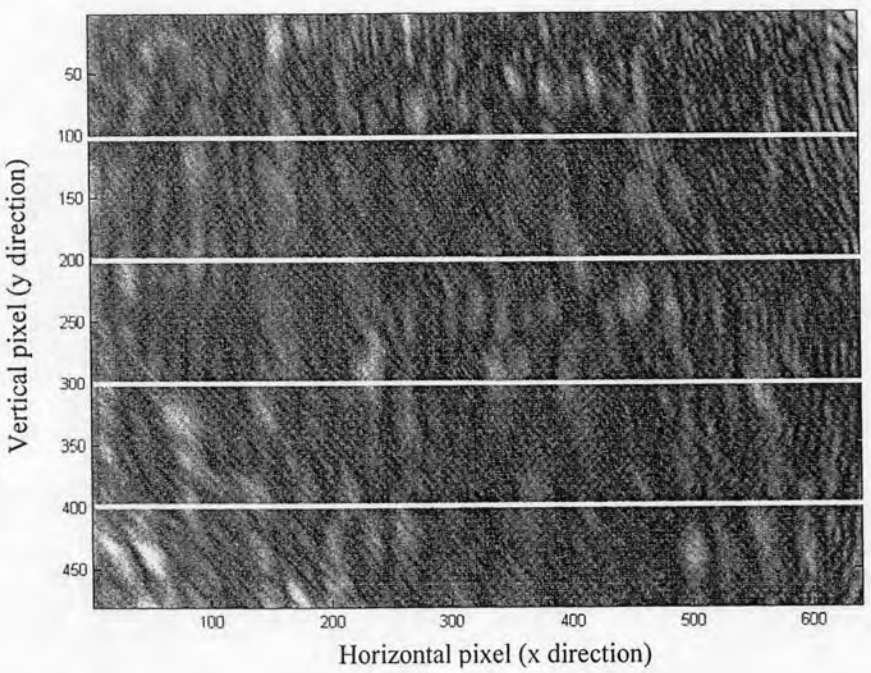

(c)

Figure 4.7: Selection lines for constructing cross-section and surface image of Sample (a) No.1 (b) No.2 and (c) No.3

4.3.1 Cross-section images of Sample No.1

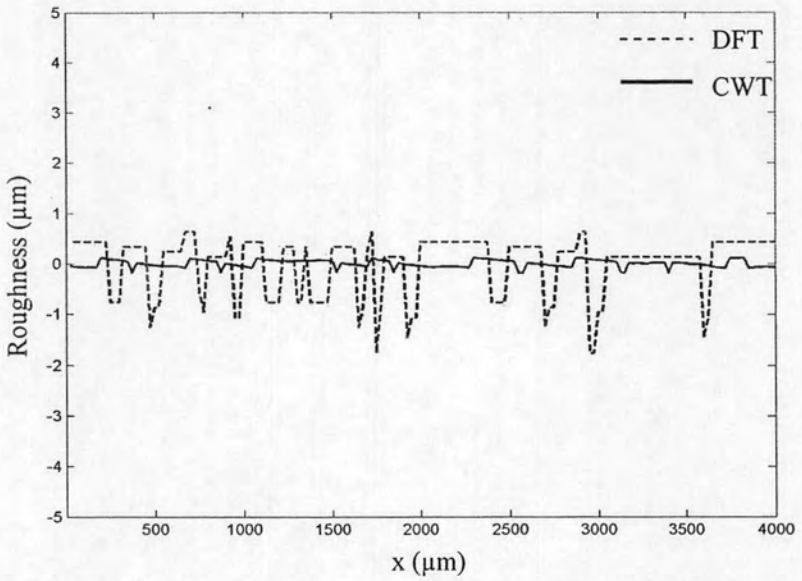

(a)

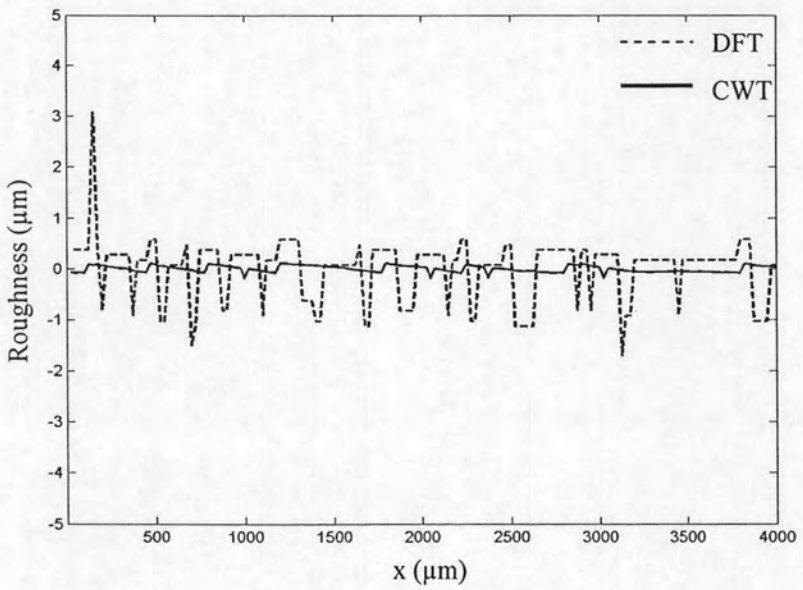

(b)

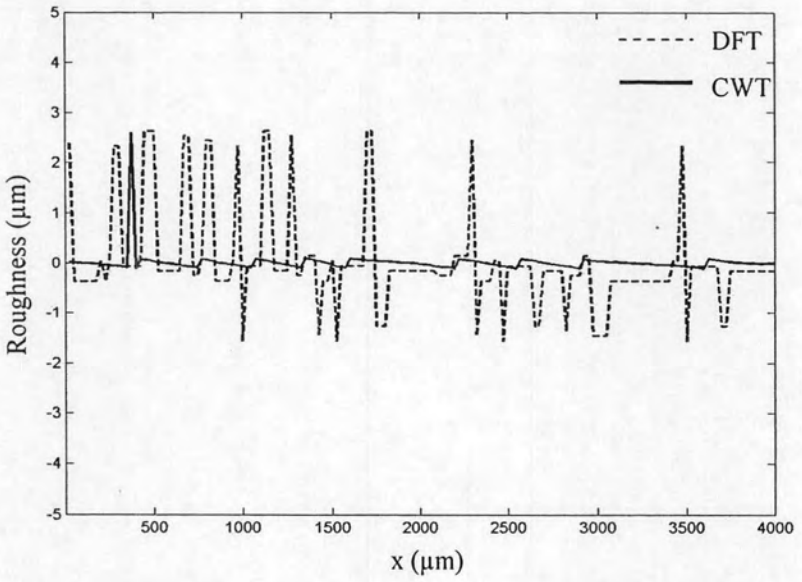

(c)

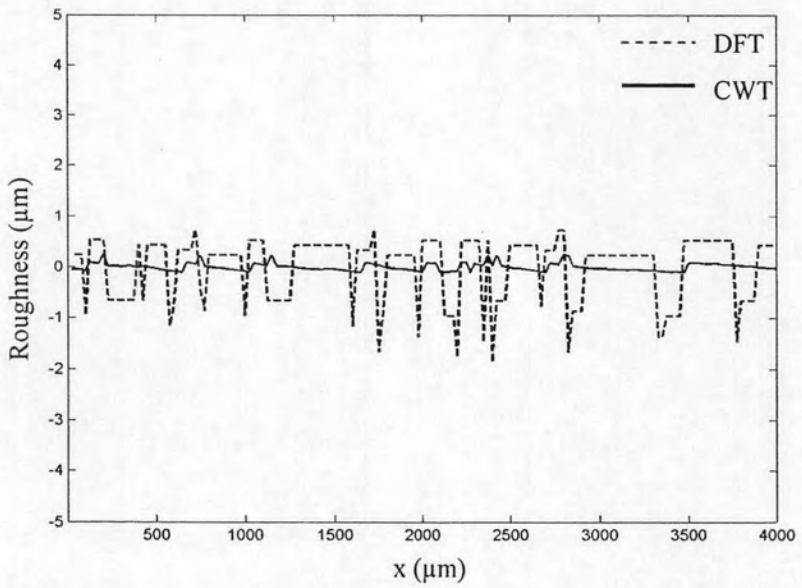

(d)

Figure 4.8: Cross-section of Sample No.1 in (a) line 1 (b) line 2 (c) line 3 and (d) line 4

Table 4.3: R_q of Sample No.1

Distances in x axis (μm)	R_q of line 1 (μm)		R_q of line 2 (μm)		R_q of line 3 (μm)		R_q of line 4 (μm)	
	DFT	CWT	DFT	CWT	DFT	CWT	DFT	CWT
1-500	0.579	0.074	0.749	0.066	1.281	0.104	0.580	0.068
501-1000	0.577	0.068	0.648	0.070	1.264	0.097	0.544	0.064
1001-1500	0.585	0.045	0.567	0.063	1.076	0.123	0.532	0.082
1501-2000	0.759	0.073	0.577	0.056	1.057	0.099	0.687	0.081
2001-2500	0.490	0.074	0.484	0.073	0.761	0.131	0.889	0.068
2501-3000	0.787	0.084	0.690	0.069	0.569	0.123	0.662	0.081
3001-3500	0.246	0.074	0.568	0.037	0.777	0.031	0.662	0.056
3501-4000	0.523	0.072	0.540	0.067	0.354	0.087	0.613	0.084
Mean	**0.568**	**0.071**	**0.603**	**0.063**	**0.892**	**0.099**	**0.646**	**0.073**

From Table 4.3, R_q from CWT were better than the one from DFT. By comparing the calculated R_q in every line, every R_q were nearly the same value. Thus, the surface of this sample was smooth. An average R_q of this sample by DFT and CWT were 0.677 μm and 0.077 μm, respectively.

4.3.2 Cross-section images of Sample No.2

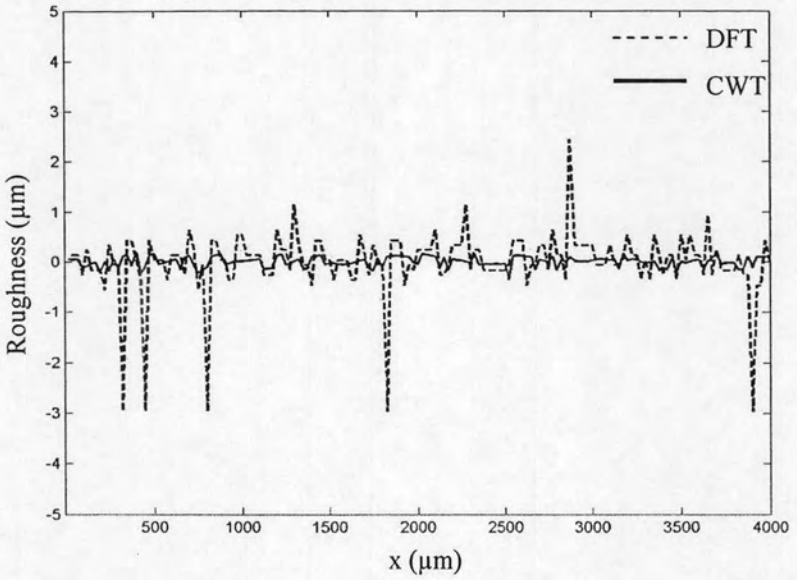

(a)

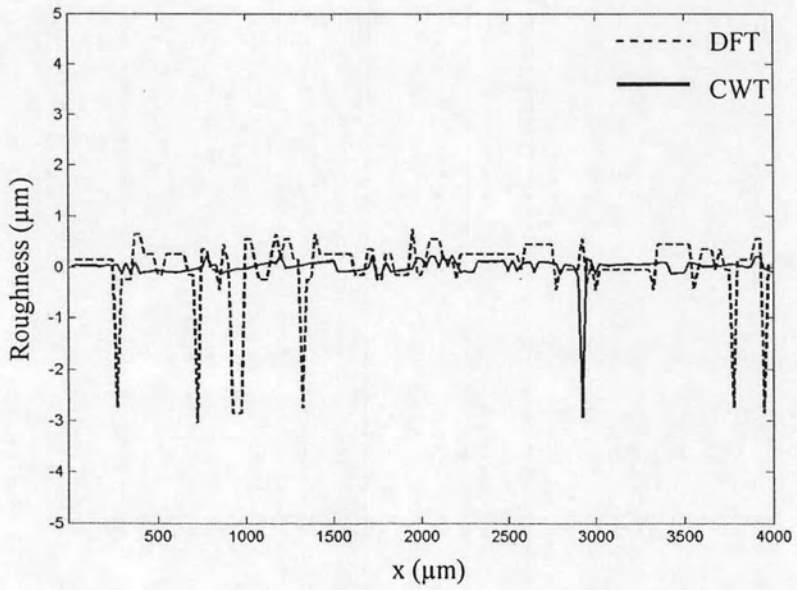

(b)

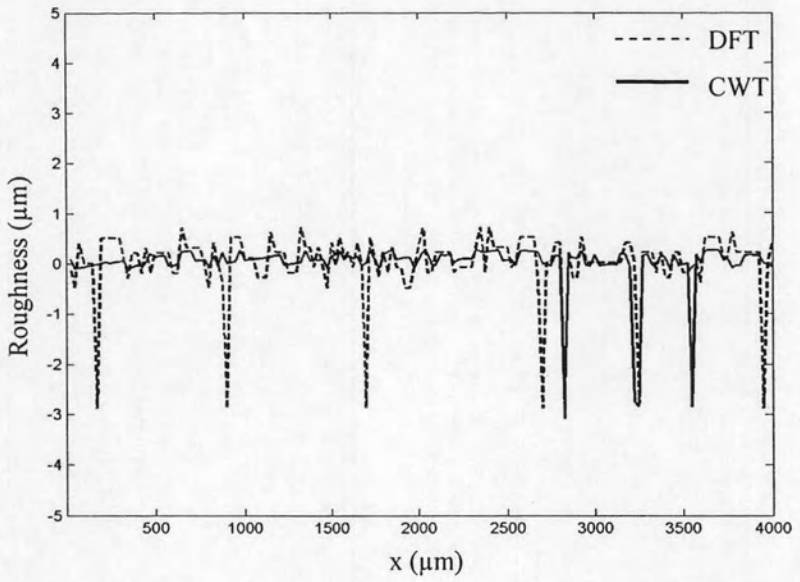

(c)

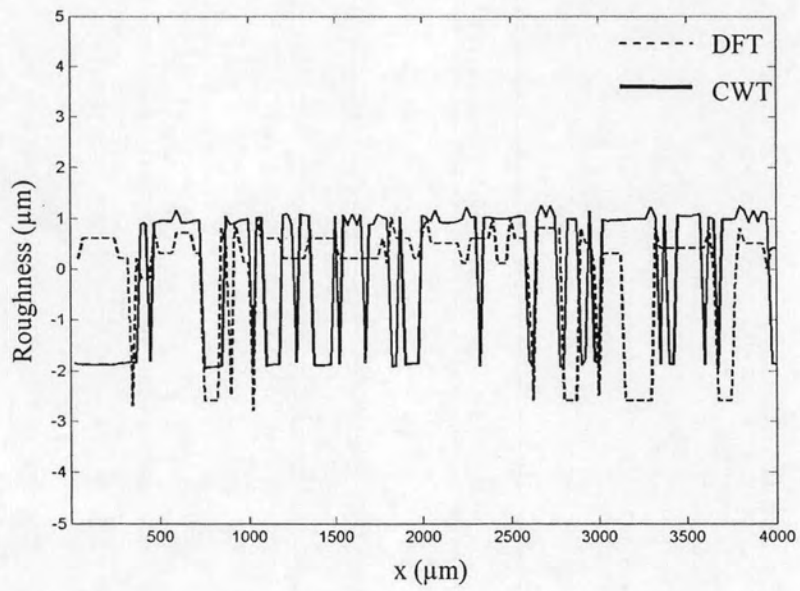

(d)

Figure 4.9: Cross-section of Sample No.2 in (a) line 1 (b) line 2 (c) line 3 and (d) line 4

Table 4.4: R_q of Sample No.2

Distances in x axis (μm)	R_q of line 1 (μm)		R_q of line 2 (μm)		R_q of line 3 (μm)		R_q of line 4 (μm)	
	DFT	CWT	DFT	CWT	DFT	CWT	DFT	CWT
1-500	0.961	0.128	0.689	0.075	0.742	0.117	0.741	0.087
501-1000	0.758	0.103	1.265	0.078	0.754	0.102	1.375	0.096
1001-1500	0.364	0.098	0.725	0.056	0.325	0.082	0.769	0.054
1501-2000	0.734	0.090	0.276	0.108	0.717	0.083	0.244	0.064
2001-2500	0.355	0.093	0.172	0.115	0.305	0.100	0.290	0.111
2501-3000	0.582	0.118	0.327	0.672	1.009	0.098	1.513	0.125
3001-3500	0.281	0.096	0.274	0.074	0.669	0.674	1.468	0.076
3501-4000	0.747	0.092	0.945	0.072	0.739	0.116	1.251	0.112
Mean	**0.598**	**0.102**	**0.584**	**0.156**	**0.657**	**0.172**	**0.956**	**0.091**

From Table 4.4, R_q from CWT were better than the one from DFT. By comparing the calculated R_q in every line, every R_q were nearly the same value but a difference of these values was more than Sample No.1. Then, this sample was rougher than Sample No.1. An average R_q of this sample by DFT and CWT were 0.700 μm and 0.130 μm, respectively.

4.3.3 Cross-section images of Sample No.3

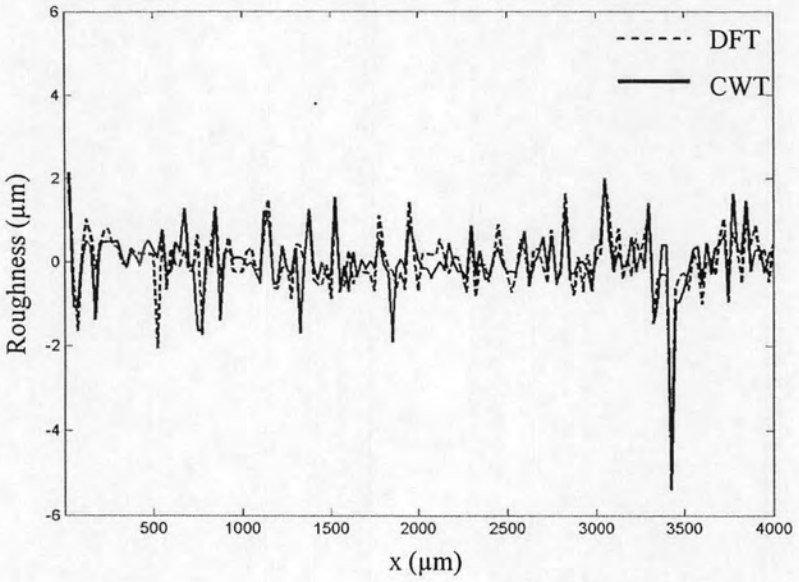

(a)

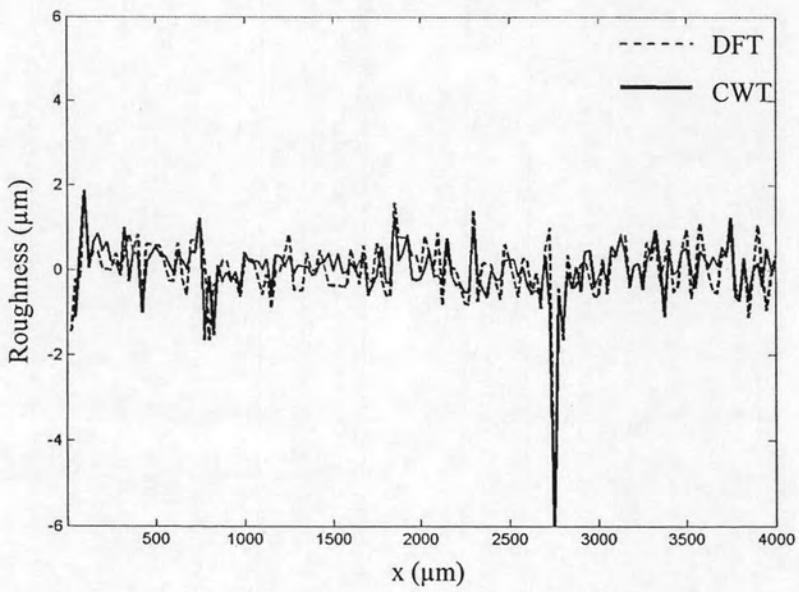

(b)

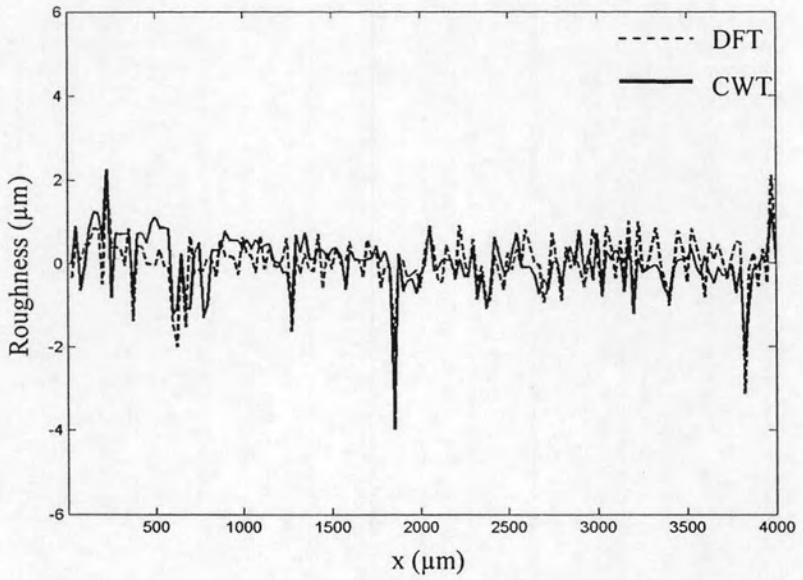

(c)

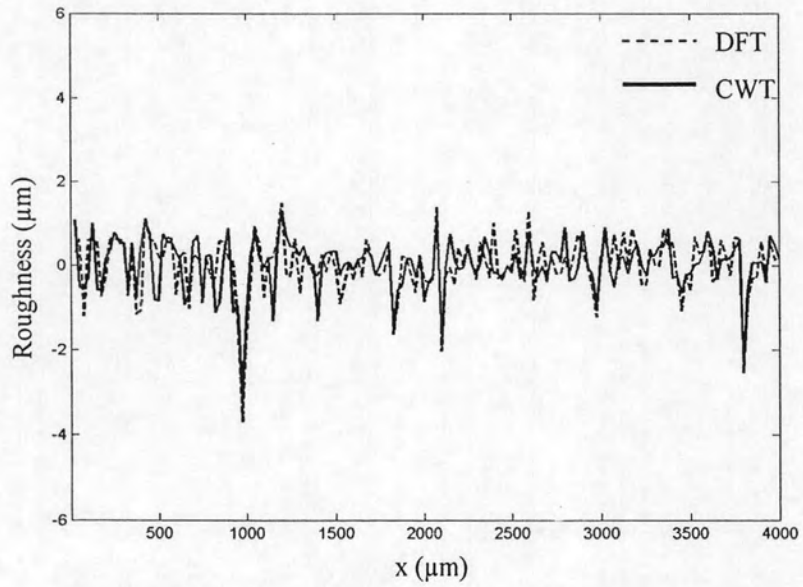

(d)

Figure 4.10: Cross-section of Sample No.3 in (a) line 1 (b) line 2 (c) line 3 and (d) line 4

Table 4.5: R_q of Sample No.3

Distances in x axis (μm)	R_q of line 1 (μm)		R_q of line 2 (μm)		R_q of line 3 (μm)		R_q of line 4 (μm)	
	DFT	CWT	DFT	CWT	DFT	CWT	DFT	CWT
1-500	0.650	0.745	0.715	0.723	0.664	0.765	0.719	0.697
501-1000	0.786	0.782	0.594	0.630	0.745	0.827	0.991	0.949
1001-1500	0.635	0.653	0.429	0.226	0.502	0.441	0.532	0.597
1501-2000	0.650	0.676	0.613	0.453	0.535	0.913	0.499	0.479
2001-2500	0.412	0.345	0.614	0.430	0.495	0.444	0.694	0.598
2501-3000	0.599	0.485	1.564	1.516	0.501	0.471	0.556	0.446
3001-3500	1.420	1.424	0.490	0.479	0.667	0.460	0.524	0.409
3501-4000	0.620	0.602	0.620	0.474	0.960	0.658	0.735	0.698
Mean	**0.722**	**0.714**	**0.705**	**0.616**	**0.634**	**0.622**	**0.656**	**0.609**

From Table 4.5, R_q from CWT were closed to DFT. That caused by a rough surface of this sample. An average R_q of this sample by DFT and CWT were 0.679 μm and 0.640 μm, respectively.

These sample were re-measured R_q by 3-D Non-Contact Surface Profiler SP-500 Series from Toray Engineering Co., Ltd. A comparison of an average R_q from SP-500 Series and this OCT method is shown in Table 4.6 and then the average R_q of Sample No.1, No.2 and No.3 by SP-500 Series, DFT and CWT is shown in Figure 4.11.

Table 4.6: Average R_q from SP-500 Series and OCT

Sample No.	Average R_q (μm)		
	SP-500 Series	DFT	CWT
1	0.065 ± 0.015	0.677 ± 0.064	0.077 ± 0.064
2	0.084 ± 0.018	0.700 ± 0.064	0.130 ± 0.064
3	0.121 ± 0.025	0.679 ± 0.064	0.640 ± 0.064

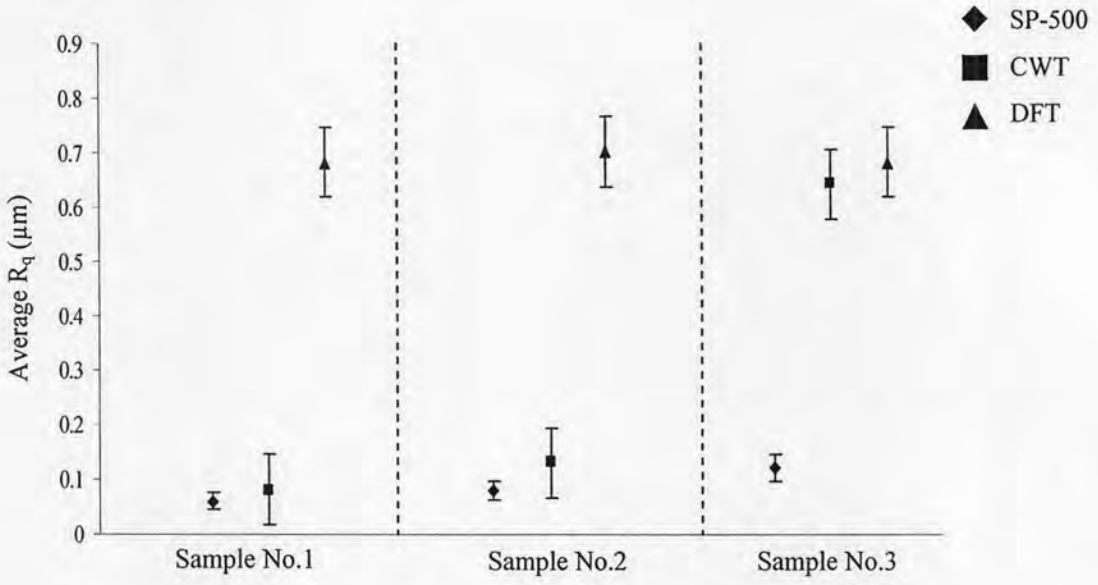

Figure 4.11: Average R_q of SP-500 Series, DFT and CWT

The average R_q of Sample No.1 and No.2 by using CWT was closed to the one by using SP-500 Series, used as standard instrument, while the average R_q of Sample No.3 by using CWT was different from the one by using standard instrument. This error came from intensity of the SLD, scattering surface and analyzing method. The intensity of the SLD affected to collimate light beam by lens. For high intensity light, the effect from the lens, Newton's ring, could be eliminated easily by using a pinhole. In this research, the SLD, used as the light source, had only 17.5 mW power; so, the effect from the lens was partially eliminated. When the light beam reflected from the sample surface, there was a scattering of light due to a roughness of the surface. Hence, the backscattered light in some areas was also too weak to detect by the CCD camera. These kinds of error had an effect on a construction of the cross-section because OCT constructed the surface height of the sample by using the intensity of backscattered light. The error of constructed surface had an effect on the R_q that was calculated by cross-section.

A method of SP-500 Series, which focuses the light beam to a random area of the surface by using the Michelson interferometer, is a main reason of a difference in R_q of CWT and SP-500 series. For smooth surface, such as the surface of standard mass, a size of light beam and a random area of measurement have not influence on R_q. While the samples, used in this research, were well polished by a common machine in a workshop, their surface was not steady smooth like the standard. That means a beam

size and a selection area would affect to R_q. Because the beam size of the parallel beam method is larger than the one by focused beam method. Thus, the parallel beam method obtained a wilder area of the surface than SP-500 Series. In the other word, the area, observed by SP-500 Series, had less a difference of peak and valley. Therefore, R_q of OCT were more than the one of the focus method.

4.4 Surface Profile of Stainless Steel Plate with and without Transparent Cover

From manufacture data, CCD camera had 640 × 480 pixels. Since a size of light beam, recorded by this CCD camera, was 4 × 3mm, each pixel of this CCD camera contained an area size of 6.25 × 6.25 μm. An effect of a flare light from neighbor CCD pixel could be reduced by considering an average of 4 × 4 pixels as a surface area. Thus, each surface area had a size of 25 × 25 μm.

A random area, which had a size of 500 × 500 μm, was chosen from the whole area of image in order to construct the surface profile of three stainless steel plates (Sample No.1, No.2 and No.3) by using CWT. Then, the surface profiles of the same area, was covered with transparent material, cover slide, were constructed and they were compared with the uncovered surface. A comparison of surface with transparent material and the one without transparent material of these samples is shown in Figure 4.12-4.17.

4.4.1 Surface profile of Sample No.1

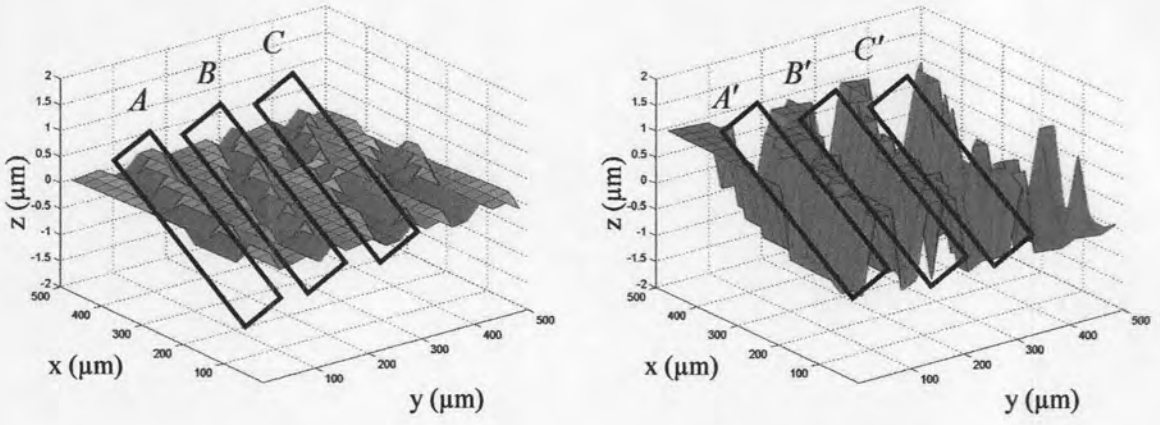

(a) (b)

Figure 4.12: Surface profile of Sample No.1 (a) without cover slide and (b) with cover slide in area 1

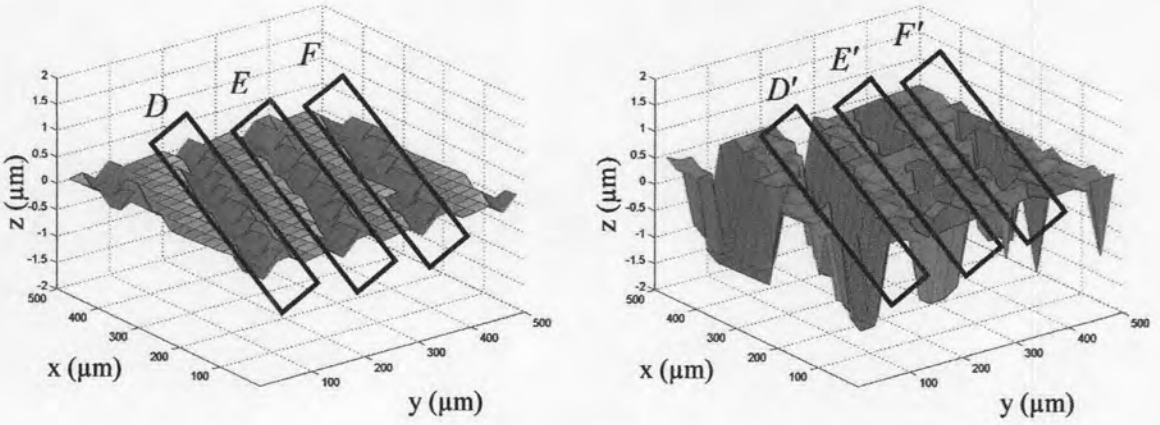

(a) (b)

Figure 4.13: Surface profile of Sample No.1 (a) without cover slide and (b) with cover slide in area 2

For Sample No.1, the area A, B and C of uncovered surface looked similar with the area A', B' and C' of covered surface and the area D, E and F of uncovered surface looked similar with the area D', E' and F' of covered surface.

4.4.2 Surface profile of Sample No.2

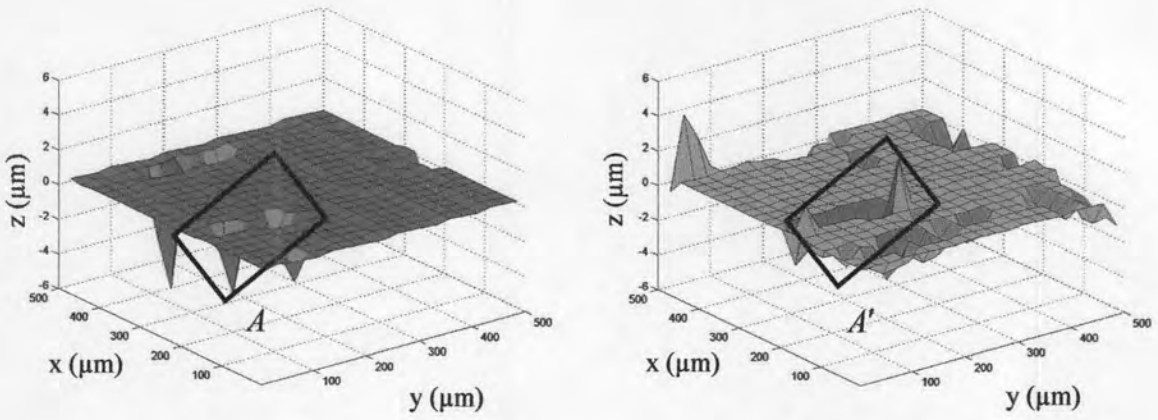

Figure 4.14: Surface profile of Sample No.2 (a) without cover slide and (b) with cover slide in area 1

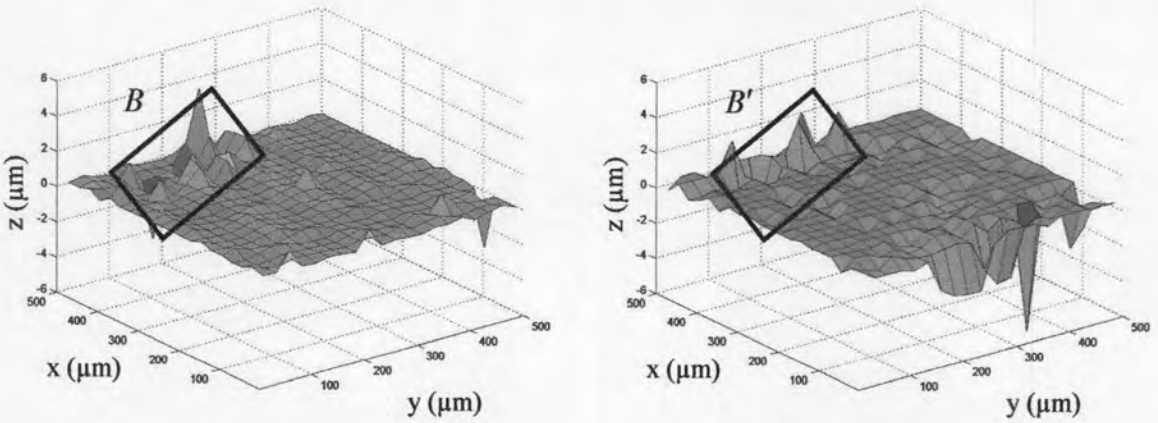

Figure 4.15: Surface profile of Sample No.2 (a) without cover slide and (b) with cover slide in area 2

For Sample No.2, the area A of uncovered surface looked similar with the area A' of covered surface and the area B of uncovered surface looked similar with the area B' of covered surface. The other area of the covered surface was also as smooth as the

uncovered surface. An error in some point might be caused by the surface of cover slide itself.

4.4.3 Surface profile of Sample No.3

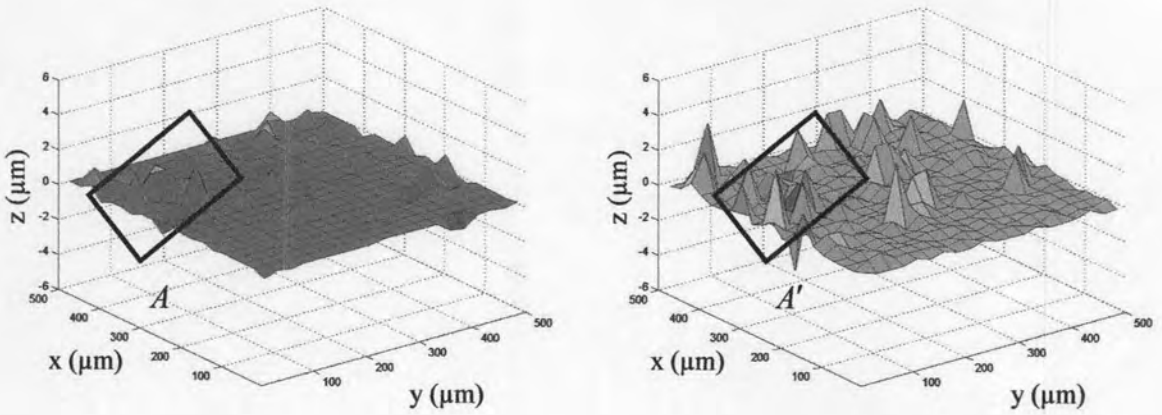

(a) (b)

Figure 4.16: Surface profile of Sample No.3 (a) without cover slide and (b) with cover slide in area 1

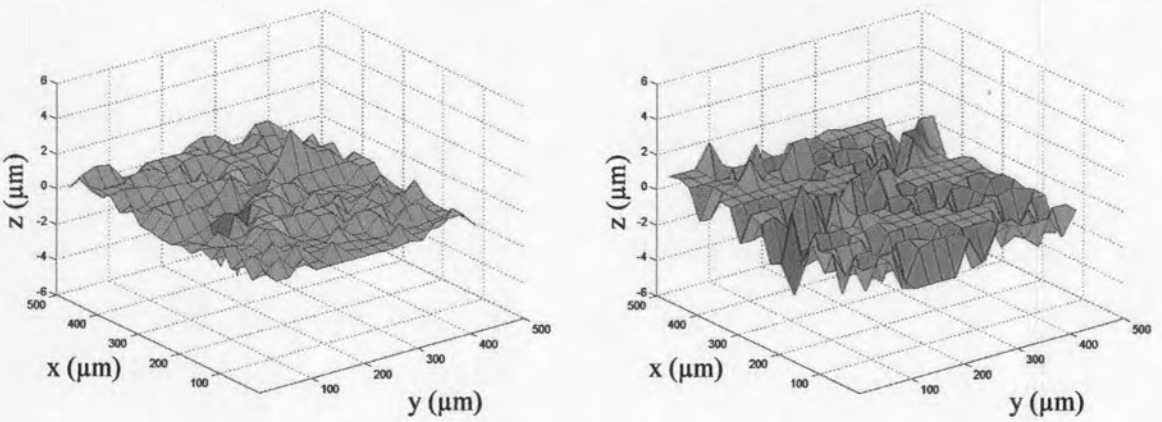

(a) (b)

Figure 4.17: Surface profile of Sample No.3 (a) without cover slide and (b) with cover slide in area 2

For Sample No.3, the area A of uncovered surface looked similar with the area A' of covered surface. In area 2, the surface of this area was not uniform; so, the covered surface was also not uniform.

The results from these samplees showed that the images of transparent cover surface were similar with the images of real surface. An error in some points might be from cover slide surface. Because the surface of the cover slide was not clear and smooth in every area, thus, an effect of the intensity of the backscattered light could be occurred and this effect had an influence on the constructed surface. R_q in area 1 and area 2 of these samples with covered and uncovered surface are shown in Table 4.7 and a comparison of R_q of covered and uncovered surface is shown in Figure 4.18.

Table 4.7: R_q of covered and uncovered surface in area 1 and area 2

Sample No.	R_q in area 1 (μm)		R_q in area 2 (μm)	
	Uncovered surface	Covered surface	Uncovered surface	Covered surface
1	0.100 ± 0.064	0.655 ± 0.064	0.101 ± 0.064	0.613 ± 0.064
2	0.290 ± 0.064	0.535 ± 0.064	0.321 ± 0.064	0.556 ± 0.064
3	0.249 ± 0.064	0.567 ± 0.064	0.481 ± 0.064	0.955 ± 0.064

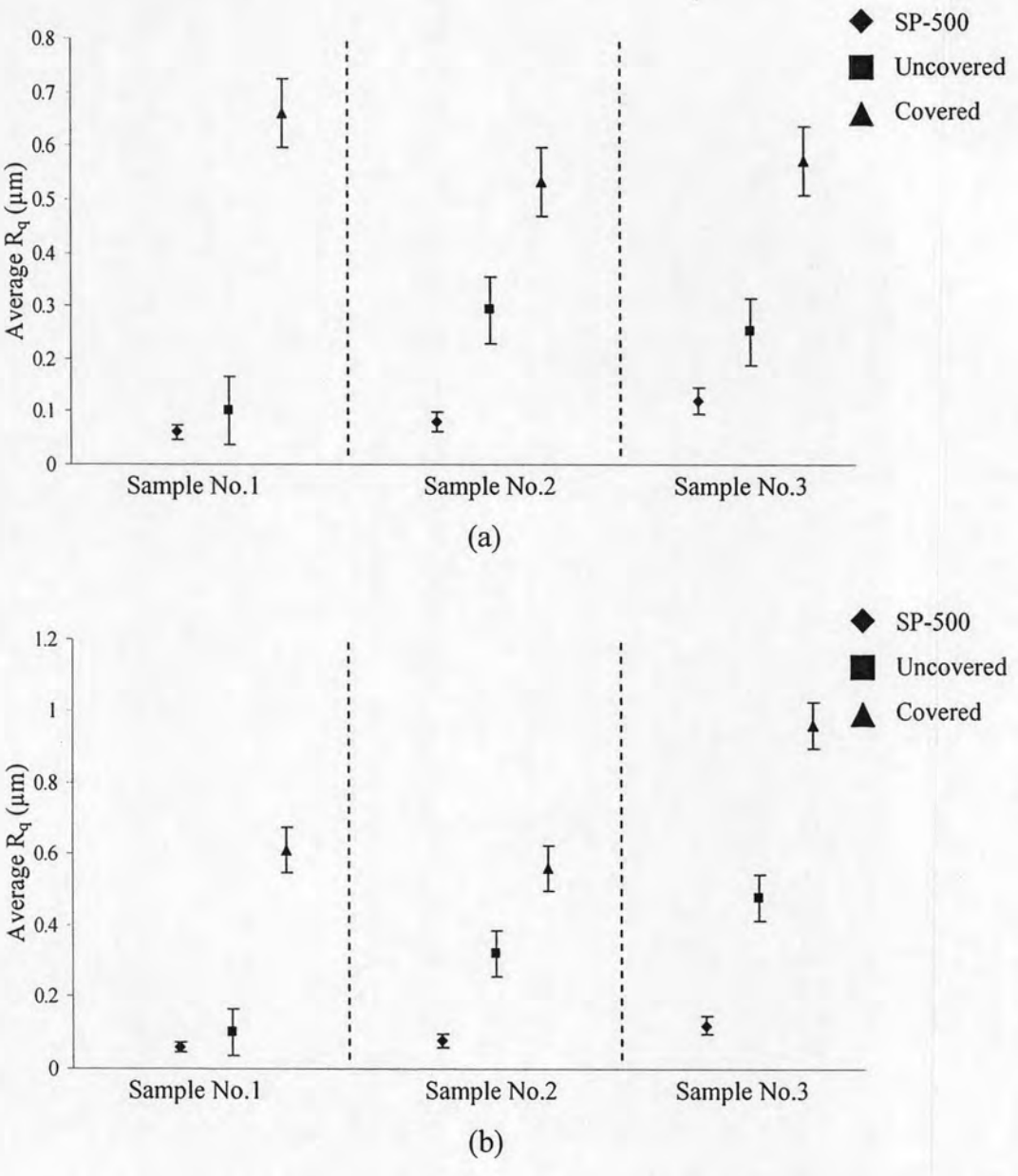

Figure 4.18: Average R_q of covered and uncovered surface in (a) area 1 and (b) area 2

R_q of covered surface were difference from uncovered surface. A difference might be from air gaps between cover slide surface and the sample surface. To avoid an error from the air gaps, the transparent material must be completely seal to the sample surface, such as a film on a substrate. In this case, the light beam will pass through the transparent material and then it directly reflects from the sample surface. Thus, the effect of the band gaps will not occur and the error in R_q will be reduced. With this method, non-uniform of an interface area between thin film surface and substrate surface may be defined.

4.5 Thickness of Cover Slide

When a sample surface is covered with transparent material, such as cover slide, interference patterns can be observed as two different positions that come from cover slide surface and stainless steel surface, used as substrate in this surface. Thus, thickness of this cover slide can be calculated by correcting this different position with the refractive index of cover slide. In case a low intensity light, a backscattering light from cover slide surface is too weak to be detected by CCD camera, then, only one interference patterns from stainless steel surface can be observed. Because a velocity of light in the cover slide decreases from its value in the air due to the refractive index of this cover slide, there is a shift in observed position of the interference patterns from the stainless steel surface with and without transparent cover. Then, the thickness of the cover slide can be calculated by this shift position, as expressed in Eq. (2.32). In this experiment, first surface height of real surface of stainless steel plate No.1, which had a smooth surface, was calculated. Next, the cover slide was placed on stainless steel plate No.1 (Sample No.1) and surface height in this case was also defined and then the thickness of the cover slide would be calculated. The differences between these surface height positions with and without transparent cover and the thickness of the cover slide in vertical pixel of 101^{st}-104^{th} (line 1), 201^{st}-204^{th} (line2), 301^{st}-304^{th} (line 3) and 401^{st}-404^{th} (line 4) are shown in Figure 4.19-4.22.

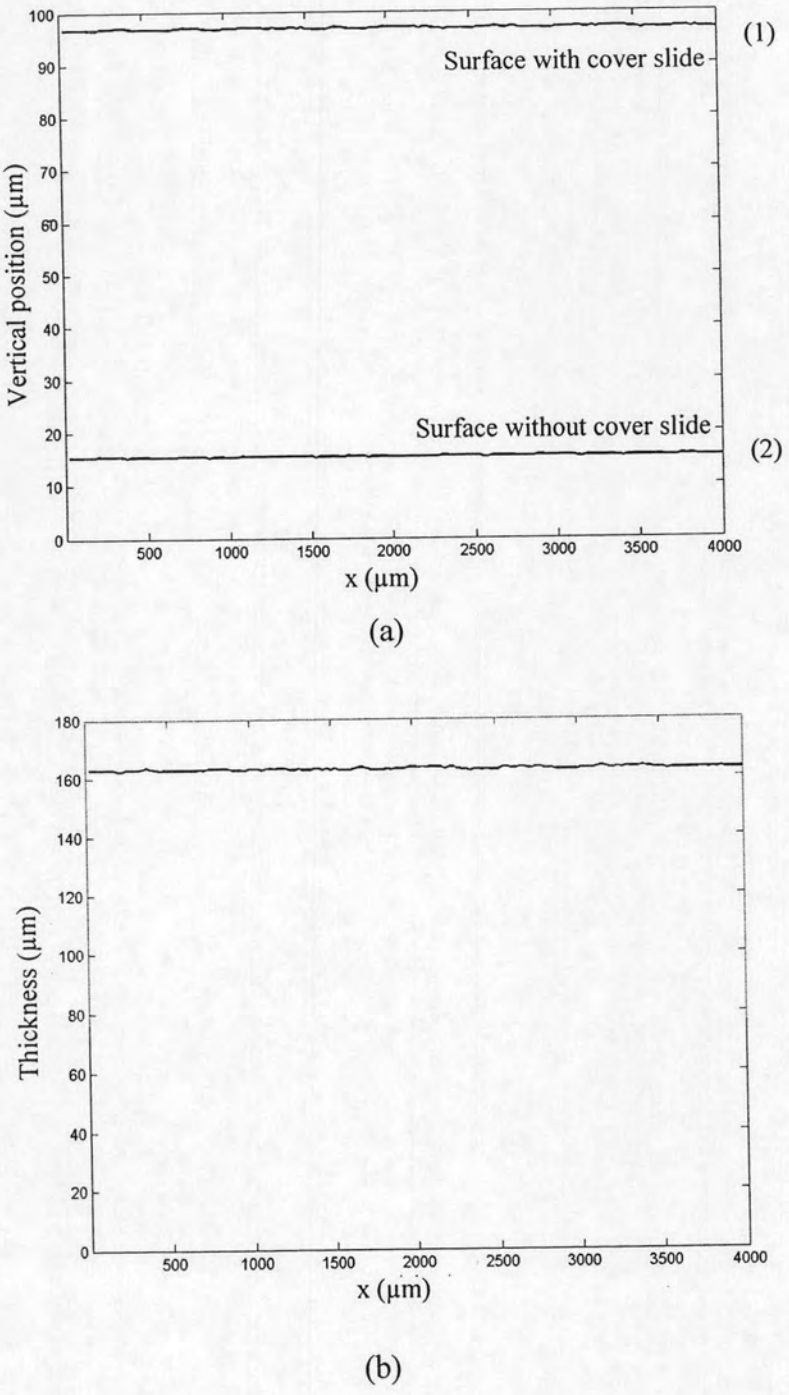

Figure 4.19: (a) Surface height with cover slide (1) and without cover slide (2) and (b) thickness of cover slide in line 1

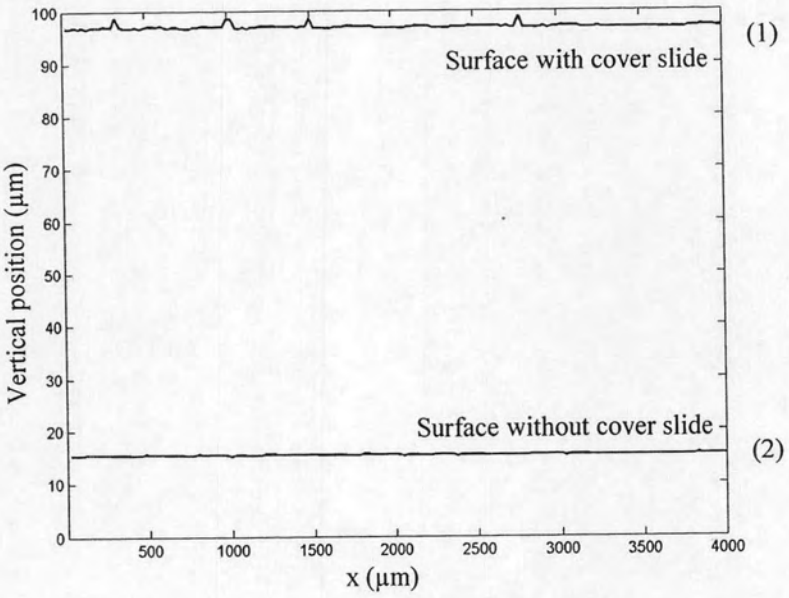

(a)

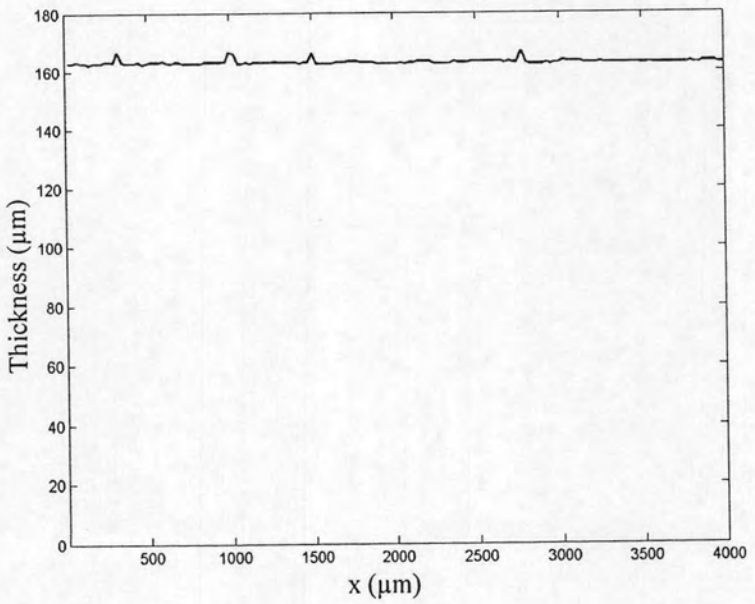

(b)

Figure 4.20: (a) Surface height with cover slide (1) and without cover slide (2) and (b) thickness of cover slide in line 2

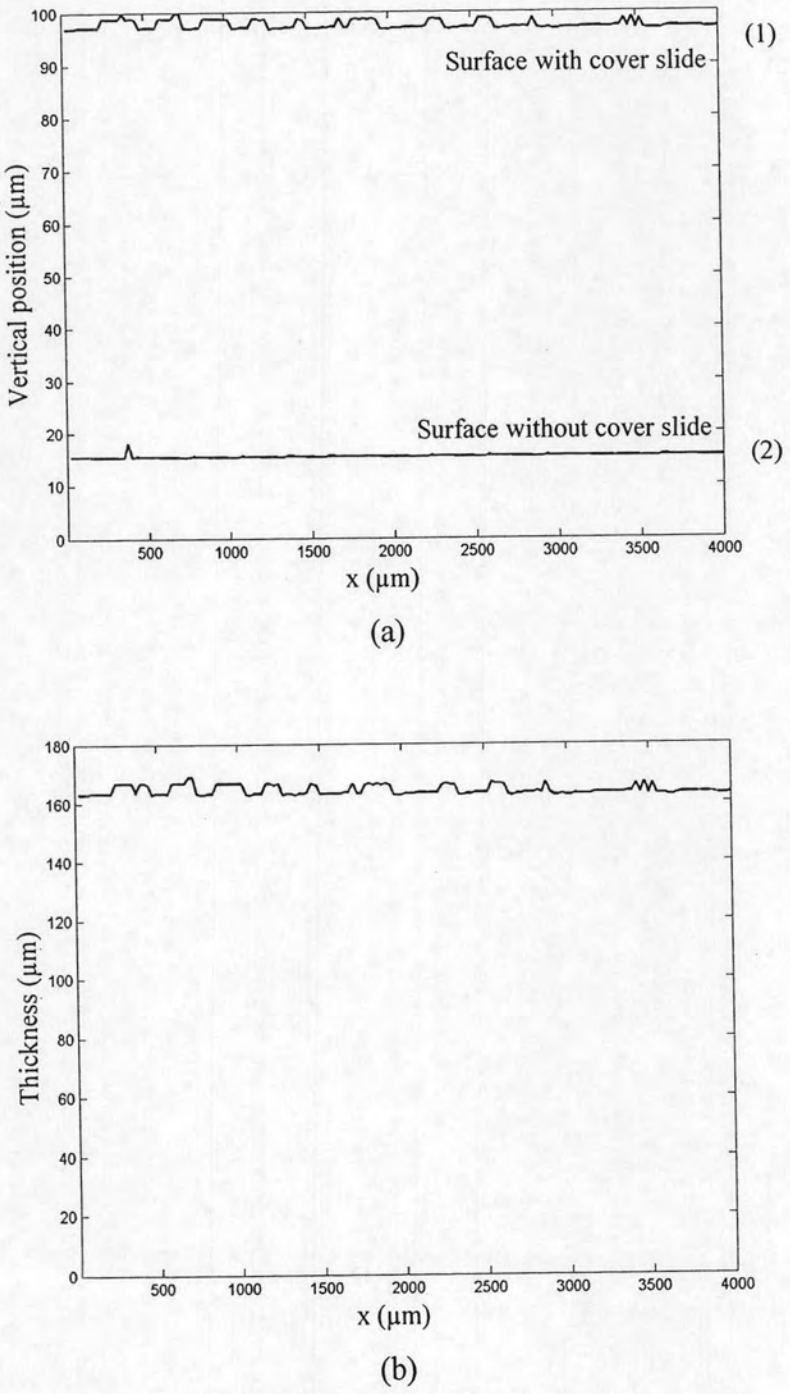

Figure 4.21: (a) Surface height with cover slide (1) and without cover slide (2) and (b) thickness of cover slide in line 3

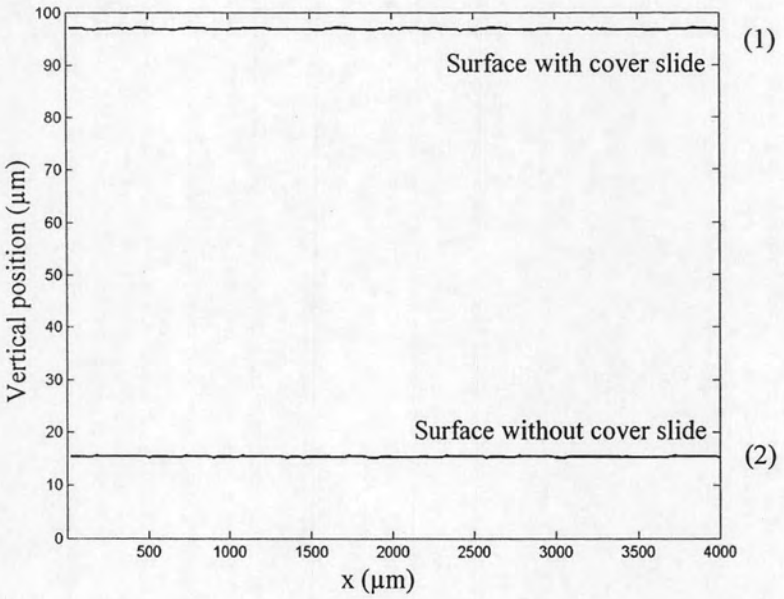

(a)

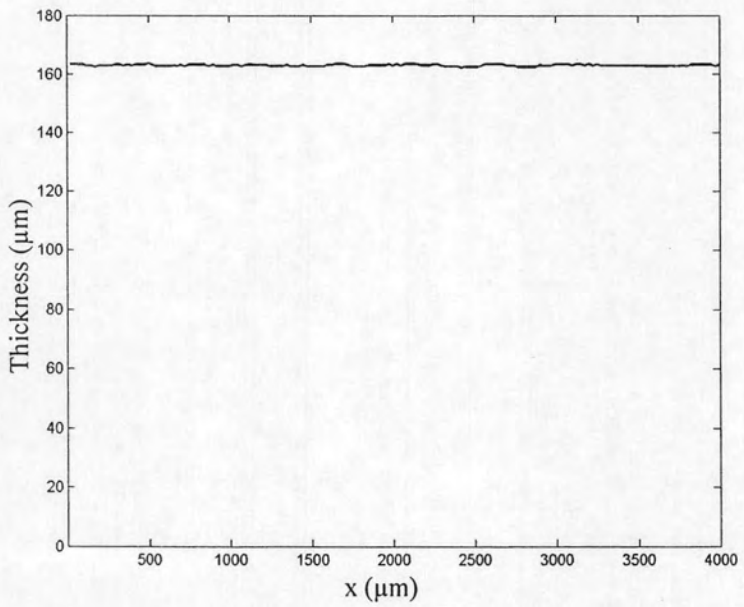

(b)

Figure 4.22: (a) Surface height with cover slide (1) and without cover slide (2) and (b) thickness of cover slide in line 4

An average thickness of cover slide in line 1, line 2, line 3 and line 4 is shown in Table 4.8 and average thickness of this cover slide, measured by length measuring instrument ULM RUBIN 800 of MAHR METROLOGY, is shown in Table 4.9.

According to the results in Table 4.8 and Table 4.9, the average thickness of the cover slide, calculated by OCT, was 163.298 ± 0.064 μm while the average thickness of this cover slide, measured by ULM RUBIN 800 Series, was 162.95 ± 0.30 μm.

Table 4.8: Thickness of cover slide in line 1, line 2, line 3 and line 4

Distances in x axis (μm)	Thickness of line 1 (μm)	Thickness of line 2 (μm)	Thickness of line 3 (μm)	Thickness of line 4 (μm)
1-500	162.888	163.141	164.633	163.100
501-1000	162.926	163.271	165.516	162.941
1001-1500	162.991	163.380	164.317	162.925
1501-2000	162.960	162.936	164.406	162.996
2001-2500	162.986	163.007	163.827	162.952
2501-3000	162.918	163.178	163.923	162.935
3001-3500	163.153	163.001	163.524	163.007
3501-4000	162.789	162.896	163.172	162.948
Mean	**162.951**	**163.101**	**164.165**	**162.974**
Average				**163.298**
System uncertainty				**0.064**

Table 4.9: Thickness of cover slide by using ULM RUBIN 800 Series

Area	1	2	3	4	5	**Average**	**Calculated uncertainty**
Thickness (μm)	160.49	162.06	163.61	167.52	161.09	**162.95**	**0.30**

By comparing the results from these two methods, the thickness of cover slide by using both ULM RUBIN 800 Series and the OCT method were difference but the uncertainty range of these values overlap. Thus, OCT has an efficiency to calculate the thickness of cover slide. From Eq.(2.32), the thickness of cover slide also depends on the refractive index of it; so, the more accuracy of the refractive index can give a good result of the thickness. From the result, this OCT method can be applied to measure the thickness of thin-layer of transparent material that its surface rarely reflects light.